Translational Oncology
www.transonc.com

Volume 10 Number 5 October 2017 pp. 806–817 806

The Functional Roles of the *MDM2* Splice Variants *P2-MDM2-10* and *MDM2-Δ5* in Breast Cancer Cells

Johanna Huun*, Liv B. Gansmo*, Bård Mannsåker*,†,1, Gjertrud T. Iversen†, Jan Sommerfelt-Pettersen‡, Jan Inge Øvrebø§,2, Per E. Lønning*,† and Stian Knappskog*,†

*Section of Oncology, Department of Clinical Science, University of Bergen, Bergen, Norway
†Department of Oncology, Haukeland University Hospital, Bergen, Norway; ‡Joint Medical Services, Norwegian Armed Forces, Sessvollmoen, Norway; §Department of Biology, University of Bergen, Bergen, Norway

Abstract

BACKGROUND: MDM2 is a negative regulator of p53 and is upregulated in numerous human cancers. While different *MDM2* splice variants have been observed in both normal tissues and malignant cells, their functions are poorly understood. *METHODS:* We evaluated the effect of *MDM2* splice variants by overexpression in MCF-7 cells and analyses of expression of downstream genes (qPCR and Western blot), subcellular localization (immunofluorescence), cell cycle assays (Nucleocounter3000), apoptosis analysis (Annexin V detection), and induction of senescence (β-galactosidase analysis). *RESULTS:* In a screen for *MDM2* splice variants in MCF-7 breast cancer cells, extended with data from healthy leukocytes, we found P2-MDM2-10 and MDM2-Δ5 to be the splice variants expressed at highest levels. Contrasting MDM2 full-length protein, we found normal tissue expression levels of P2-MDM2-10 and MDM2-Δ5 to be highest in individuals harboring the promoter SNP309TT genotype. While we detected no protein product coded for by MDM2-Δ5, the P2-MDM2-10 variant generated a protein markedly more stable than MDM2-FL. Both splice variants were significantly upregulated in stressed cells ($P = 4.3 \times 10^{-4}$ and $P = 7.1 \times 10^{-4}$, respectively). Notably, chemotherapy treatment and overexpression of P2-MDM2-10 or MDM2-Δ5 both lead to increased mRNA levels of the endogenous MDM2-FL ($P = .039$ and $P = .070$, respectively) but also the proapoptotic gene *PUMA* ($P = .010$ and $P = .033$, respectively), accompanied by induction of apoptosis and repression of senescence. *CONCLUSION:* We found P2-MDM2-10 and MDM2-Δ5 to have distinct biological functions in breast cancer cells. *GENERAL SIGNIFICANCE:* Alternative splicing may influence the oncogenic effects of the *MDM2* gene.

Translational Oncology (2017) 10, 806–817

Introduction

The E3 ubiquitin ligase MDM2 is a negative regulator of the p53 tumor suppressor protein [1,2]. MDM2 binds and ubiquitinates p53, facilitating it for proteasomal degradation [3,4]. p53, on the other hand, can induce transcription of *MDM2*, generating a negative feedback loop [5,6]. *MDM2* gene amplification and/or protein overexpression have been implicated in various types of cancer and been suggested to be an alternative mechanism of p53 inactivation [2,7,8]. *MDM2* is expressed from two separate promoters, promoter P1 and P2, initiating various transcripts with different translational potential [9,10]. Transcription from P1 is

Address all correspondence to: Stian Knappskog, Section of Oncology, Department of Clinical Science, University of Bergen, N-5020, Bergen, Norway.
E-mail: stian.knappskog@uib.no
[1] Current address: Department of Oncology and Palliative Medicine, Bodø, Norway.
[2] Current address: Huntsman Cancer Institute, University of Utah Health Care, USA.
Received 19 June 2017; Revised 27 July 2017; Accepted 27 July 2017

1936-5233/17
http://dx.doi.org/10.1016/j.tranon.2017.07.006

known to be essential in most unstressed cells, while transcription from P2 is considered to be triggered by increased p53 activity under stressed conditions [10,11].

Two SNPs within the *MDM2* intronic promoter P2, SNP309T > G (rs2279744) and SNP285G > C (rs117039649), have been found to be associated with altered *MDM2* expression [12,13]. Both SNPs affect the binding of the transcription factor Sp1 [12,13]. While the minor allele of SNP309 (G) extends the Sp1 binding site, and several studies have associated the G variant with elevated risk for different cancer forms [12,14,15], the minor allele of SNP285 reduces Sp1 binding and has been related to a reduced cancer risk [13,16,17]. The potential impact of these promoter SNPs on the expression of *MDM2* splice variants has, so far, not been investigated.

The *MDM2* gene consists of 12 exons, coding for a full-length protein harboring 491 amino acids [18]. The protein contains a p53 binding domain at the N-terminal and a highly conserved RING domain responsible for the E3 ligase activity at the C-terminal in addition to an NLS, an NES, and an NoLS [19–22], allowing the protein to be localized both in the nucleus and in the cytoplasm [23] (Figure 1).

MDM2 is expressed as several alternatively and aberrantly spliced transcripts. The first alternative spliced *MDM2* transcripts were identified in human tumors almost two decades ago [24]. To the best of our knowledge, 72 different *MDM2* splice variants are described in human cancers and normal tissue to date [18,25–27].

We selected the P2-MDM2-10 and MDM2-Δ5 variants for in-depth analyses based on an initial screen of MCF-7 cells and lymphocytes from healthy young males. In addition, treatment of MCF-7 cells with chemotherapy induced significantly elevated expression levels of both these splice variants.

Material and Methods

Blood Sample Donors

RNA used for expression analyses was extracted from white blood cells drawn from 216 healthy young males as part of a routine test during compulsory service in the Norwegian navy [28]. Prior to RNA extraction, the white blood cells from each individual were divided into two fractions; one half was irradiated (3 Gy) and the other half was kept untreated.

DNA and RNA Extraction

Genomic DNA from leukocytes was extracted using the Qiagen DNA mini-kit according to the manufacturer's instructions. Total RNA was extracted using Trizol reagent (Life technologies) according to the manufacturer's instructions, and cDNA synthesis was performed as previously described [28].

MDM2 Splice Variant Screening

In P2-MDM2-10, the first 15 bases of exon 10 are retained, while the rest of exon 10 is spliced out, resulting in a protein of 476 amino acids. Previous studies have indicated P2-MDM2-10 to be expressed from promoter P2 only [25]. MDM2-Δ5 is an aberrantly spliced variant of the *MDM2* transcript that lacks exon 5. The deletion of this exon leads to a shift in the reading frame of the mRNA transcript. The resulting open reading frames potentially cause expression of two different proteins of 9.8 kDa and 76 kDa (Figure 1).

MDM2 transcripts were amplified with nested PCR using forward primer specific for either promoter P1 or P2.

Promoter P1 was amplified by 5′-GAAGGAAACTGGGGAGTC TTG-3′ and 5′-GACTCC AAGCGCGAAAAC-3′.

Promoter P2 was amplified by 5′-GTGTTCAGTGGCGATTGG AGG-3′ and 5′-AGACCTGTGGGCACGGA-3′.

The reverse primers were the same for both P1 and P2: 5′-GAGAAAATGCCTCAATTCACATAG-3′ and 5′-CTATATAA CCCTAGGAATTTAGACAA-3′.

PCR conditions are given in detail in Supplementary Methods. Subsequently, the PCR products were subjected to TOPO TA Cloning (Invitrogen, Life Technologies), and positive clones were analyzed by Sanger sequencing with the following primers: P1 transcripts; 5′-ATGGTGAGGAGCAGGCAAATG and for P2 transcripts 5′-TGCTGATCCAGGCAAATGTG using BigDye Terminator v3.1 Cycle Sequencing Kit (Thermo Fisher Scientific) according to the producer's protocol.

MDM2 Promoter Genotyping

All samples were genotyped for *MDM2* SNP309 and SNP285 by Sanger sequencing as previously described [13,17].

P2-MDM2-10 and MDM2-Δ5 Expression Analysis

Quantitative PCRs of *MDM2* splice variants P2-MDM-10 and MDM2-Δ5 and the internal reference gene *RPLP2* were carried out using hydrolysis probes (TIB MOLBIOL) on a Lightcycler 480II instrument (Roche) with the following primers and probes:

P2-MDM2-10: forward 5′-CGGATCTTGATGCTGGTGTAT ATC-3′, reverse 5′-GAAGCCAATTCTCACGAAGG-3′ and probe: 5′-6FAMTCAGGCAGGGGAGAGTGATACAGA TTC-BBQ.
MDM2-Δ5: forward 5′-AGACACTTATACTATGAAAG AGGAAAAT-3′, reverse 5′-TGACACCTGTTCTCACTC and probe: 5′-6FAM-AGCAGGAATCATCGGACTCAGG-BBQ.
RPLP2: forward 5′-GACCGGCTCAACAAGGTTAT-3′, reverse 5′-CCCCACCAGCAGGTACAC-3′ and probe 5′-Cy5-AG CTGAATGGAAAAAACATTGAAGACGTC-BBQ.

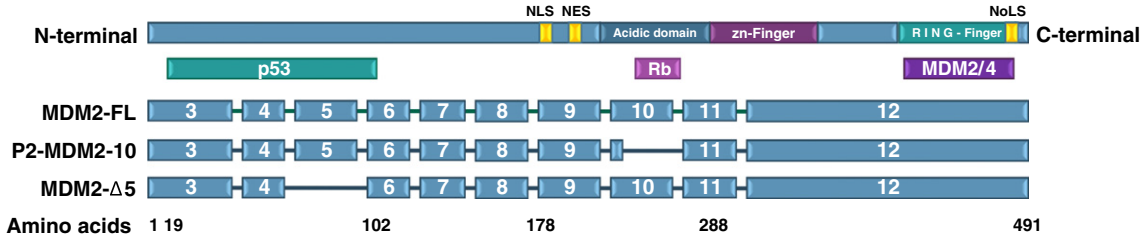

Figure 1. *MDM2* and the splice variants P2-MDM2-10 and MDM2-Δ5. MDM2-FL consists of 491 amino acids; localization of the p53, pRb and MDM2/4 binding sites, NLS, NES, NoLS, the acidic domain, the Zn-finger domain, and the RING-finger domain is indicated on in the two top panels. Exons included in MDM2-FL as well as P2-MDM2-10 and MDM2-Δ5 are indicated in the three bottom panels.

Amplifications were performed in a reaction volume of 10 μl using the LightCycler 480 Probes Master kit (Roche) with 0.5 μM of each primer pair, 0.125 μM of probe and 3 μl cDNA. The two-step qPCR cycling conditions were: 5-minute initial denaturation at 95°C before 50 cycles of 10 seconds at 95°C and 25 seconds at annealing temperature, followed by a cooling step at 40°C for 10 seconds. The annealing temperatures were 59°C for P2-MDM2-10, 57°C for MDM2-Δ5, and 53°C for *RPLP2*.

MDM2-FL Expression Analysis

Cells were transfected and sorted by Flow Cytometry (FACS Aria) based on GFP expression. Six hours post seeding, the cells were treated with DMSO or 1 μM doxorubicin for 12 hours. The total RNA was isolated from the cells using Trizol reagent (Life Technologies, Gaithersburg, MD) according to the manufacturer's instructions. Single-stranded cDNA synthesis was performed using 500 ng total RNA, oligo-dT, and random hexamer primers (Sigma) with Transcriptor Reverse Transcriptase (Roche) in accordance with manufacturer's instructions. Levels of mRNAs were determined individually with the following primers and probes (TIB MOLBIOL):

EXON3 was amplified with the primers 5′-AACATGTCTGTACCTACTGATGGTGC-3′ and 5′-CAGGGTCTCTTGTTCCGAAGC-3′ and the hydrolysis probe 6FAM-AACCACCTCACAGATTCC-BBQ.
3′UTR was amplified with the primers 5′-TGCTCCATCACCCATGCTAGA-3′ and 5′-TGGT GGTACATGCCTGTAATC-3′ and the hydrolysis probe 6FAM-TAGCTTGAACCCAGAAGGCGGA-BBQ.

RPLP2 was amplified described above. The qPCR cycling conditions were set as described above; the annealing/extension temperatures were EXON3 53°C and 3′UTR 58°C. Quantitative amplification reactions were performed with custom-made Realtime Ready plates (Roche; Configurator no. 100,054,567) on the LightCycler 480 instrument (Roche) using the same reaction conditions as described above.

Specificity Tests for Expression Assays

In order to validate the specificity of the splice variant–specific qPCR assays, we first normalized the concentration of a plasmid containing the splice variant (P2-MDM2-10 or MDM2-Δ5) to the exact same concentration as a plasmid containing the MDM2 WT. This was done by running qPCRs targeting shared MDM2 regions in the plasmids and then adjusting the concentrations until identical Cp values were reached. These reactions were performed using the following primes and probes (TIB MOLBIOL):

P2-MDM2-10/MDM2 WT: forward 5′-GACTAAACGATTATATGATGAGAAGCA-3′, reverse 5′-GCTCTTTCACAGAGAAGCTTGG-3′ and probe 6FAM-TCTTCTAGGAGATTTGTTTGGCGTG-BBQ.
MDM2-Δ5/MDM2 WT: forward 5′-TTGATGCTGGTGTAAGTGAACA-3′, reverse 5′-TGAAGAAGGACAAGAACTCTCAGA-3′ and probe 6FAM-AAGTTGAATCTCTCGACTCAGAAGATTATAGCCT-BBQ.

Reactions were run with the same solutions and thermocycling conditions as described above, except that the annealing/extension temperature was set to 55°C.

Subsequently, in order to detect any potential contribution from wild-type template in the splice variant–specific qPCRs, the MDM2 WT plasmid and the splice plasmids, now having the same concentrations, together with a pooled sample of cDNA from white blood cells were analyzed by the splice variant–specific assays. Both splice variant–containing plasmids were detected within the range of the pooled cDNA from white blood cells (Cp = 28-33), while the MDM2 WT plasmid were not detected (no positive reaction curve after 50 cycles; Figure S1). Thus, the contribution from WT template in the splice-specific qPCR assays was negligible.

Expression Vectors

The sequences encoding the respective splice variants P2-MDM2-10 and MDM2-Δ5 were assembled from synthetic oligonucleotides and cloned into *E. coli* expression vectors by Geneart, (Life Technologies). *MDM2* encoding fragments were cut out using the *Bam*HI and *Xho*I restriction sites. Following agarose gel purification, the fragments were ligated into a pCMV eukaryotic expression vector (CMV-MCS-V5-6xHis-BGHpolyA in pCMV-cyto-EGFP-myc) using T4 DNA ligase. The utilized vector contained a sequence encoding an eGFP expressed from an independent CMV promoter region. Performing immunofluorescence, apoptosis, and senescence analysis, a pcDNA3.1V5-vector (TOPO) was used, providing a C-terminal V5-tag (Invitrogen). The plasmids were amplified in One Shot TOP10 Chemically Competent *E. coli* cells (Invitrogen) by ampicillin selection followed by colony PCR and purified using the QIAprep Spin Miniprep Kit (Qiagen). The constructed plasmids encoding MDM2-FL and splice variants were confirmed and checked for mutations by sequencing using the BigDye1.1 system and Sanger sequencing prior to large-scale purification from *E. coli* by the HiSpeed plasmid maxi kit (Qiagen) according to the manufacturer's instructions. The resulting stock solutions of the plasmids were validated by sequencing to ensure absence of any mutations prior to introduction to a eukaryotic cell system.

Cell Culture, Transfection, and Treatment

The cells were fingerprinted with AmpFISTR Profiler and Cofiler plus (Applied Biosystems by Life Technologies) prior to use. MCF-7 (HTB-22) breast cancer cells (ATCC) were cultivated in EMEM (ATCC) supplemented with 10% FBS, 2% L-glutamine, and 2% penicillin streptavidin (Lonza). HCT116 (CCL-247) colon cancer cells (a generous gift from Dr. Fred Bunz, Bert Vogelstein, and Kenneth W. Kinzler at John Hopkins University and Howard Hughes Medical Institute, MD) were cultivated in McCoy's medium (ATCC) supplemented with 10% FBS, 0.12% gentamycin, and 2% penicillin streptavidin (Lonza). Transfection was performed using 1.85 μg/ml of each plasmid (pCMV-P2-MDM2-10, pCMV-MDM2-Δ5, pCMV-MDM2-FL, pCMV) and 1.7 μl/ml Lipofectamine 2000 (Invitrogen). As negative control, cells were treated with DMSO at the same amount as for the corresponding chemotherapy-treated cells with 1 μM doxorubicin in DMSO. Both DMSO and doxorubicin were diluted in cell growth medium before application to the cells.

Sorting Cells by Flow Cytometry and GFP Transfection Efficiency

GFP transfection efficiency was measured after all transfections using the NucleoCounter3000 instrument (Chemometec). Twelve hours posttransfection, the cells were harvested and sorted by Flow Cytometry (FACS Aria) based on eGFP expression. The sorted cells were immediately seeded in new growth medium and further assessed

in various assays. The transfection efficiency was measured consecutively to be on average 31% for P2-MDM2-10 and 34% for MDM2-Δ5 (data not shown).

Western Blot Analysis

Cells were harvested with Trypsin EDTA (Lonza) and lysed with IPH buffer with protease inhibitor, debris were removed, and proteins were denatured by boiling in SDS buffer and loaded on 12% SDS-PAG (Bio Rad) with PS11 protein ladder (GeneOn). Separated proteins were transferred onto 0.2-μM nitrocellulose membranes by turbo blotting for 7 minutes, 2.5A, and 25 V using the Bio Rad system. Unspecific protein binding was blocked by incubation in 5% nonfat milk in TBS-Tween$_{0.05\%}$ for 1 hour at room temperature or overnight at 4°C. Membranes were subsequently incubated in MDM2 specific antibody Sc-813 (Santa Cruz) recognizing exon 3. Potentially expressed proteins from MDM2-Δ5 were investigated using different antibodies having their epitope in exon 3 (Sc 813, Santa Cruz), exon 8 (Sc-965, Santa Cruz), and exon 12 (OP 146, Merck Millipore), respectively. GAPDH (SantaCruz) was used as loading control. Following washing of membranes in TBS-Tween$_{0.05\%}$, proteins bound by the primary antibody were detected by HRP-conjugated secondary antibody (Sigma). Signals were detected using SuperSignal West Femto Chemiluminescent Substrate (Thermo Scientific) and the LAS 4000 imager (GE Healthcare).

Protein Stability Analysis

Twenty-four hours posttransfection, the cells were treated with DMSO or 1 μM doxorubicin for 24 hours. The cells were then exposed to 100 μg/ml cycloheximide (Sigma) and harvested after 1, 2, and 4 hours. Cells were washed (ice-cold PBS), deattached (Trypsin-EDTA), and neutralized (EMEM) followed by centrifugation and subsequent washing of the generated cell pellet in cold PBS. Proteins were released by cell lysis for 10 minutes in IPH buffer with protease and phosphatase inhibitors. Cell debris was removed by centrifugation at 13,000 rpm for 1 minute. Protein concentration was measured by absorption measurements at 280 nm using the NanoDrop2000 (Thermo Scientific). By varying the amount of cell lysate, equal amount of total protein was denatured in sodium dodecyl sulfate sample buffer and boiled at 95°C for 5 minutes, followed by Western blotting. GAPDH (Santa Cruz) was chosen as loading control due to its high stability over time. All experiments were performed in triplicate.

Subcellular Localization by Indirect Immunofluorescence

Cells were grown on glass coverslips and transfected as previously described. Forty-eight hours after transfection, the cells were fixed for 15 minutes in 3.7% formaldehyde. Cells were then permeabilized with 0.1% Triton X-100 for 10 minutes and blocked with 1% BSA in PBS for 30 minutes. The coverslips were then incubated with MDM2 specific antibody Sc-813 (Santa Cruz) for 1 hour followed by AlexaFluor 647–conjugated secondary antibody (Life Technologies) for 30 minutes. The cells were incubated 10 minutes in 0.1% Hoechst 33,342 (Molecular Probes, Life Technologies) in PBS, washed in 1× PBS, and mounted with Fluka Eucitt quick hardening mounting solution (Life Technologies). Fluorescent cells were observed with a confocal laser scanning microscope (Leica TCS SP5, Leica Microsystems). Localization was determined by three individual persons who analyzed 18 representative anonymous pictures for each of the *MDM2* splice variants.

Cell Cycle Analysis

Transfected and treated cells were incubated 5 minutes at 37°C in lysis buffer with Hoechst (Chemometec). Thereafter, cells were added stabilizing buffer before analysis with the NucleoCounter 3000 (Chemometec) for DNA quantitation in three independent experiments.

Cell Proliferation by Cell Count

Cells were seeded on six-well tissue plates. Twenty-four hours after transfection, the cells were treated with DMSO or 1 μM doxorubicin for 24 hours. The cells were trypsinated and counted by NucleoCounter3000 Viability assay.

Apoptosis Assay: Annexin V Detection

Transfected cells were treated with DMSO or 1 μM doxorubicin for 24 hours before they were trypsinated and washed in 1× PBS. Further, the cells were incubated 15 minutes at 37°C in Annexin V (Biotium) and Hoechst 33,342 (Chemometec). The cells were washed once in Annexin V buffer (Biotium) before they were resuspended in Annexin V buffer with 4% propidium iodide (Chemometec) and analyzed with the NucleoCounter3000 (Chemometec) for identification of live, necrotic, and early- and late-apoptotic cells. The analysis was repeated in three independent experiments.

Senescence Assay: β-Galactosidase Staining

Transfected cells were treated with 0.25 μM doxorubicin for 7 days before staining for β-galactosidase activity with the Senescence β-galactosidase Staining Kit (Cell Signaling) according to the manufacturer's instructions; briefly, the cells were incubated in staining solution for 14 hours at 37°C without CO_2 in a cultivation incubator with humidified atmosphere. Senescent cells were detected as blue β-galactosidase–positive cells versus negative cells upon microscopic inspection (Nikon eclipse TS100).

Statistics

Splice variant expression levels were analyzed with respect to promoter SNP genotypes by Kruskal-Wallis (K-W) and Mann-Whitney (M-W) rank tests. The subcellular localization and degree of senescence were tested by χ^2 for comparison of the different groups. Interaction between apoptosis and senescence and the phase distribution in the cell cycle were tested by two-way variance analysis. All *P* values are reported as two-sided.

Results

In the present study, we assessed the potential biological functions of the MDM2 splice variants P2-MDM2-10 and MDM2-Δ5. These two variants were selected for characterization based on two criteria: First, we screened MCF-7 cells both before and after doxorubicin treatment and lymphocytes from healthy young males both before and after irradiation, and found P2-MDM2-10 and MDM2-Δ5 to be the most frequently detected *MDM2* splice variants (Figure S2). Secondly, when treating MCF-7 cells with a low dose of doxorubicin (0.1 μM), we found significantly elevated expression levels of both P2-MDM2-10 and MDM2-Δ5 as compared to the untreated control cells ($P = 4.3 \times 10^{-4}$ and $P = 7.1 \times 10^{-4}$, respectively; Figure S3). Notably, applying first exon specific (i.e., promoter usage specific) assays, we found both P2-MDM2-10 and MDM2-Δ5 to be expressed from both *MDM2* promoters (P1 and P2), yielding transcripts with different 5'UTRs but identical open reading frames given that the

start codon is located in exon 3. Comparing the expression levels within MCF-7 cells, we found the MDM2 full-length (WT) transcript to be expressed 25- and 110-fold higher than the MDM2-Δ5 and the P2-MDM2-10 transcripts, respectively (Figure S4).

MDM2 Promoter Genotypes and Normal Tissue Splice Variant Expression

To assess the relationship between promoter genotypes, previously reported to affect MDM2 transcription (defined according to SNPs 309 and 285 status) [12,13], and the expression levels of the P2-MDM2-10 and MDM2-Δ5 splice variants, we analyzed leukocytes from 216 healthy young males for whom the SNPs have previously been genotyped [13]. For six individuals, P2-MDM2-10 levels were undetectable, and these were therefore excluded from the statistical analysis.

Within these leukocyte samples, we observed a significant difference in P2-MDM2-10 as well as MDM2-Δ5 expression levels between individuals harboring the three *MDM2* SNP309 genotypes (K-W; $P = .044$ and $P = .018$ for P2-MDM2-10 and MDM2-Δ5, respectively), with individuals carrying the SNP309TT genotype having the highest expression level. Applying the recessive model (SNP309TT versus SNP309TG + GG), we observed significantly higher expression levels of both P2-MDM2-10 and MDM2-Δ5 splice variants among individuals harboring the SNP309TT as compared to individuals harboring the SNP309TG + GG genotypes (M-W $P = .044$ and $P = .005$ for P2-MDM2-10 and MDM2-Δ5, respectively; Figure 2*A*). No significant differences in splice variant expression between individuals harboring different genotypes in respect to SNP285 were observed (K-W P2-MDM2-10: $P = .90$; MDM2-Δ5: $P > .5$).

Assessing expression levels of the two splice variants in parallel leucocyte samples from the same individuals before and after exposure to 3 Gy of irradiation, we found the level of both splice variant to increase significantly (average increase of 6.27-fold for P2-MDM2-10 and 2.94-fold for MDM2-Δ5; $P = 1.3 \times 10^{-35}$ and $P = 3.5 \times 10^{-37}$, respectively; Figure 2*C*). The magnitude of the increase (relative or absolute) did not differ between individuals harboring the different SNP genotypes ($P > .3$). However, similar as to what was recorded for pretreatment samples, MDM2-Δ5 expression levels remained higher among individuals carrying the SNP309TT genotype as compared to the SNP309TG + GG genotypes after irradiation as well (M-W $P = .006$; Figure 2*B*).

Cellular Effects of P2-MDM2-10 Overexpression

Overexpression of P2-MDM2-10 in MCF-7 cells revealed a protein product of 87 kDa (Figure 3). Vector integrity and transcription were validated by qPCR (data not shown). P2-MDM2-10 protein stability

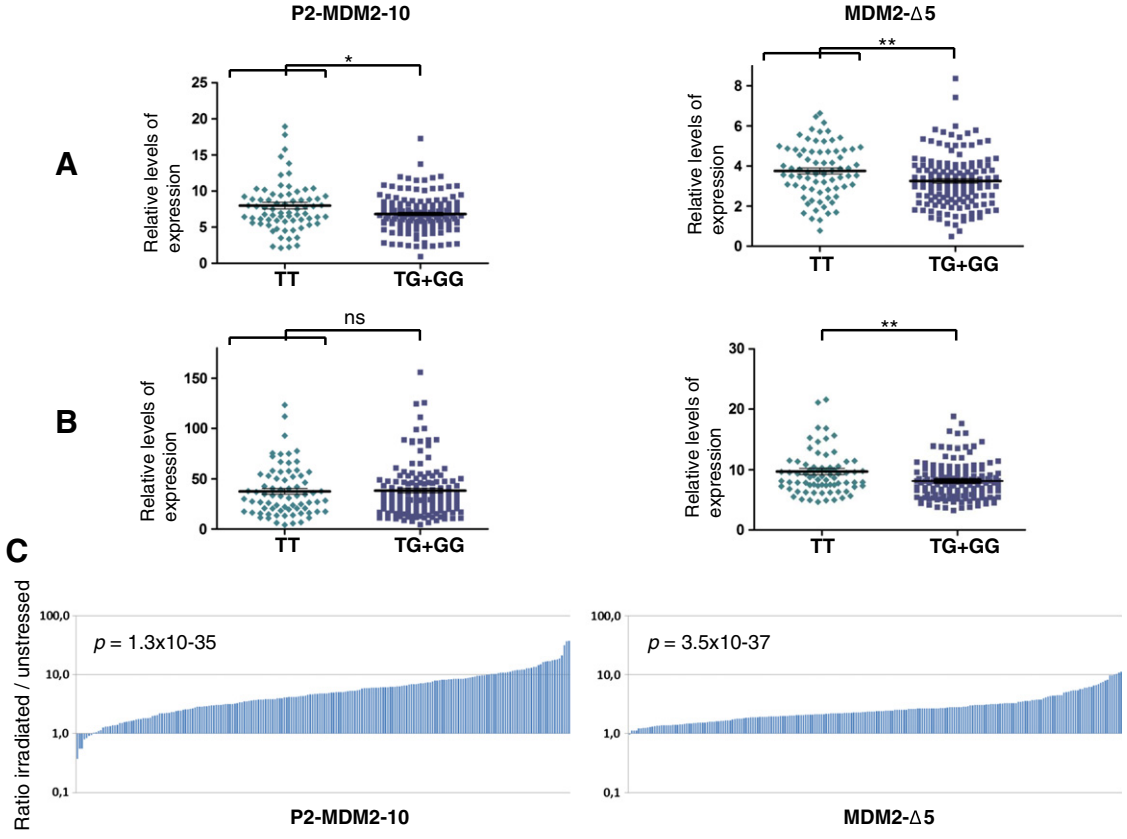

Figure 2. *MDM2* promoter genotypes and normal tissue splice variant expression. (A) Scatter plots representing the relative levels of total P2-MDM2-10 and MDM2-Δ5 mRNA in individuals carrying the *MDM2* SNP309 TT genotype versus the TG+GG genotypes in unstressed lymphocytes. *$P \leq .05$, **$P \leq .01$. *n* Δ5: TT = 75, TG = 102, GG = 39, *n* Δ10: TT = 73, TG = 101, GG = 36. (B) Scatter plots representing the relative levels of total P2-MDM2-10 and MDM2-Δ5 mRNA in individuals carrying the *MDM2* SNP309 TT genotype versus the TG + GG genotypes in irradiated (3 Gy) lymphocytes. ns = nonsignificant, **$P \leq .01$. *n* Δ5: TT = 75, TG = 102, GG = 39, *n* Δ10: TT = 73, TG = 101, GG = 36. (C) Ratio of expression levels for P2-MDM2-10 (left) and MDM2-Δ5 (right) mRNA in irradiated vs. unstressed cells.

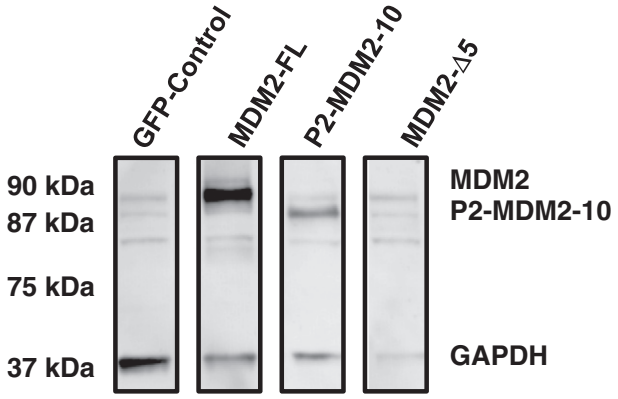

Figure 3. Protein expression after transfection. MCF-7 breast cancer cells transfected with pCMV-GFP control (GFP-control), MDM2-FL (90 kDa), P2-MDM2-10 (87 kDa), and MDM2-Δ5 were analyzed 24 hours after transfection. GAPDH (36 kDa) was used as loading control. Primary antibodies were anti-MDM2 OP146 (Merck Millipore) and anti-GAPDH (Santa Cruz).

was assessed by protein synthesis blockage using cycloheximide treatment. Interestingly, we found P2-MDM2-10 to be markedly more stable than the MDM2-FL protein both in untreated cells and, particularly, in cells subject to stress by doxorubicin treatment (Figure 4).

Regarding subcellular localization, we found P2-MDM2-10, similar to MDM2-FL, to be localized exclusively in the nucleus in the majority of cells (Figure 5*A*). However, the fraction of cells with the protein located in the exclusively in the nucleus (as opposed to the cytoplasm or both of these compartments) was significantly higher for P2-MDM2-10 than for the MDM2-FL (χ^2 test $P = .007$; Figure 5*B*).

Next, we investigated whether ectopic overexpression of P2-MDM2-10 affected the mRNA levels of a panel of p53 downstream targets as well as endogenous MDM2. Here, we used cells sorted based on eGFP expression to ensure P2-MDM2-10 overexpression in all assayed cells. We found P2-MDM2-10 overexpression to significantly upregulate the proapoptotic *BBC3* (*PUMA*) gene after doxorubicin treatment compared to both the control cells ($P = .011$) and cells overexpressing MDM2-FL ($P = .010$; Figure 6), possibly indicating a role for P2-MDM2-10 in apoptosis. Similar differences were not observed for unstressed cells. In addition, we found overexpression of P2-MDM2-10 to increase the levels of endogenous *MDM2* mRNA both in untreated and in doxorubicin-treated cells; the difference, however, was of statistical significance in cells exposed to doxorubicin only ($P = .072$ and $P = .039$, respectively; Figure 7). Notably, these differences were not detected in our protein analyses (Figure 3) probably due to the superior sensitivity of qPCR over Western blot analysis. In contrast, overexpressing P2-MDM2-10 had no effect on *MDM4, RB1, E2F1, TP53, MTOR, CDK1A, ATM, PTEN, BCL2,*

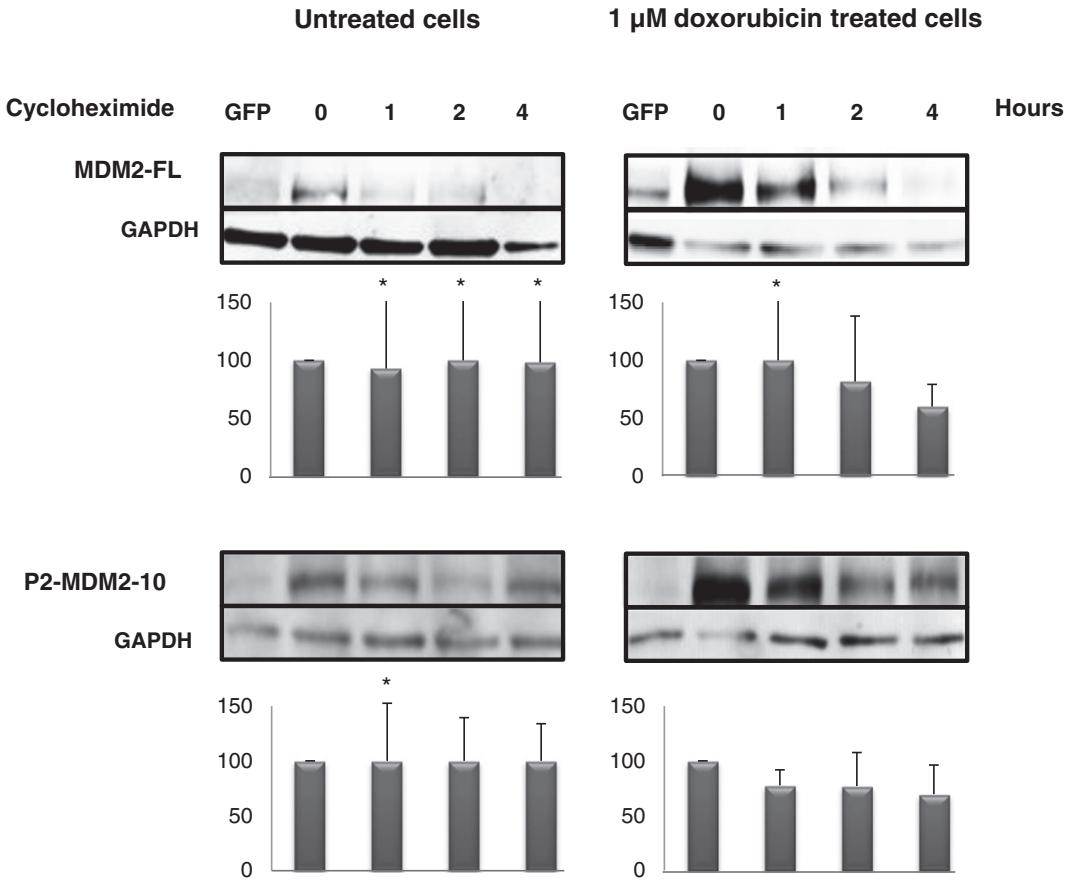

Figure 4. Protein stability of the expressed *MDM2* splice variants. MCF-7 cells transfected with P2-MDM2-10 at 0, 1, 2, and 4 hours after cycloheximide treatment. Left panel: non–doxorubicin-treated cells; right panel: cells treated with 1 μM doxorubicin for 24 hours prior to cycloheximide. Primary antibodies anti-MDM2 (N-20) Sc-813 (Santa Cruz) and anti-GAPDH (Santa Cruz). The experiment was repeated in triplicate, with three independent transfections.

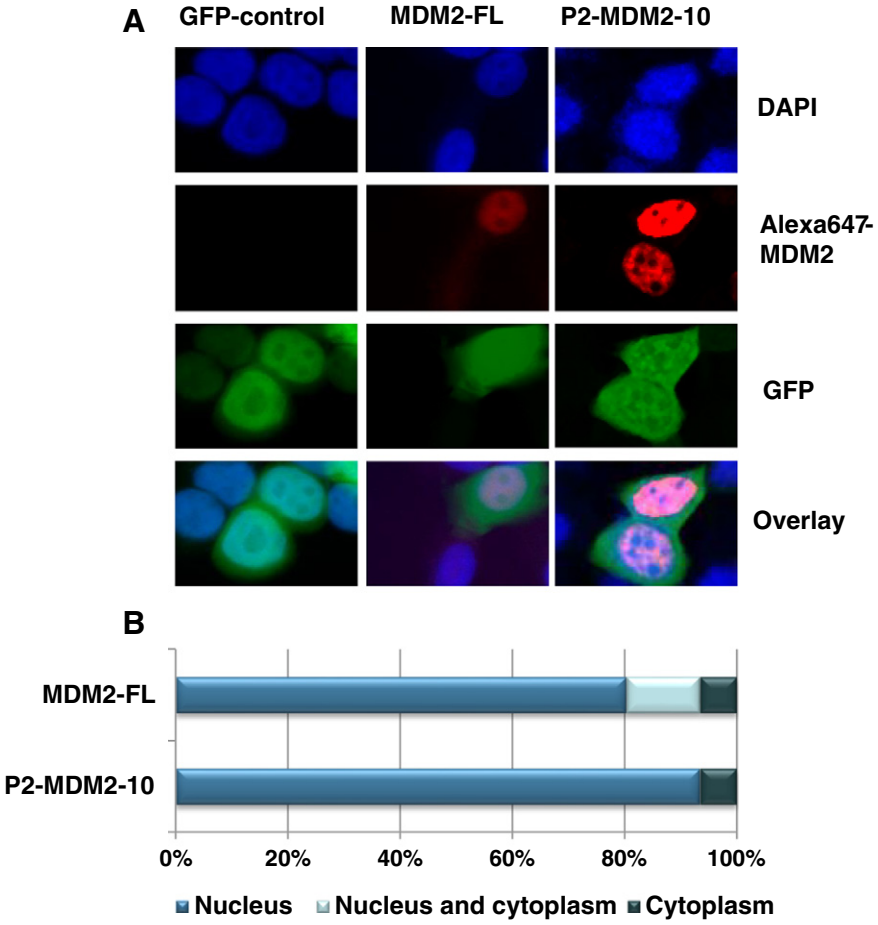

Figure 5. Subcellular localization of the *MDM2* splice variants. (A) MCF-7 cells transfected with pCMV-GFP (GFP-control), MDM2-FL, and P2-MDM2-10 evaluated by indirect immunofluorescence for determination of cellular localization of the proteins. Nuclei stained by DAPI (blue, top row); cellular compartments bound to Alexa-647 MDM2 antibody (red; second row); the cells expressing GFP (green, third row); overlay (bottom row). (B) Bars indicate the percentage of cells with exclusively nuclear (dark blue), nuclear and cytoplasmic (blue), or exclusively cytoplasmic (light blue) localization of the MDM2-FL and the P2-MDM2-10 splice variant. Subcellular localization was determined by counting >100 cells per experiment for each of the MDM2-FL and the P2-MDM2-10 splice variant. The experiment was repeated in triplicate, with three independent transfections, counted by three independent investigators.

APAF, or *GLB1* mRNA levels either in untreated cells or in cells subjected to doxorubicin treatment (data not shown).

In light of the *PUMA* induction, we investigated whether P2-MDM2-10 had an impact on cellular end points, such as cell cycle proliferation, apoptosis, or senescence. Assessing the potential impact of P2-MDM2-10 on cell cycle regulation, P2-MDM2-10 overexpression did not affect cell cycle progression in either untreated or doxorubicin-treated cells (Figure 8*A*). Although the differences were limited, we did, however, observe a slightly increased proliferation in cells overexpressing P2-MDM2-10 at 72 hours post transfection (P = .008; Figure 8*B*). Importantly, in line with the induction of *PUMA*, we found overexpression of P2-MDM2-10 to result in a marked increase of apoptotic cells compared to the TOPO-control in untreated (55% vs. 28% of cells) as well as in doxorubicin-treated cells (60% vs. 49%; Figure 9*A*). Notably, we also found an increase in apoptotic cells upon overexpression of the MDM2-FL both in the untreated as well as in the doxorubicin-treated cells.

Since this latter observation contrasts with what one might expect assuming MDM2-FL to influence apoptosis by inhibiting p53, we sought to validate this finding in other cell lines. For this purpose, we used isogenic versions of HCT116 colon cancer cells, only differing with respect to *TP53* status. Both HCT116 *TP53*–/– and +/+ revealed higher or similar degree of apoptosis when overexpressing MDM2-FL as compared to TOPO-control (Figure S5). Furthermore, HCT116 *TP53*–/– showed indications of increased activation of apoptosis upon doxorubicin treatment and overexpression of P2-MDM2-10 but not to statistical significance.

In MCF7 cells, we also assessed the impact of P2-MDM2-10 overexpression on senescence: In doxorubicin-treated cells, the increased degree of apoptosis (described above) was accompanied by a decrease in the fraction of cells undergoing cellular senescence (Figure 9*B*). In the TOPO-control cells, doxorubicin treatment lead to a 5.8-fold increase in senescence compared to the cells that are not exposed to doxorubicin. In the cells overexpressing P2-MDM2-10, the increase was found to be 4.5-fold. When comparing the increase in activated apoptosis and the reduction in senescence by univariate analysis of variance, the interaction between them was found to not reach statistical significance (P = .188).

Cellular Effects of MDM2-Δ5 Overexpression

No protein product was detected subject to overexpressing MDM2-Δ5 mRNA (see Methods section). This was not due to

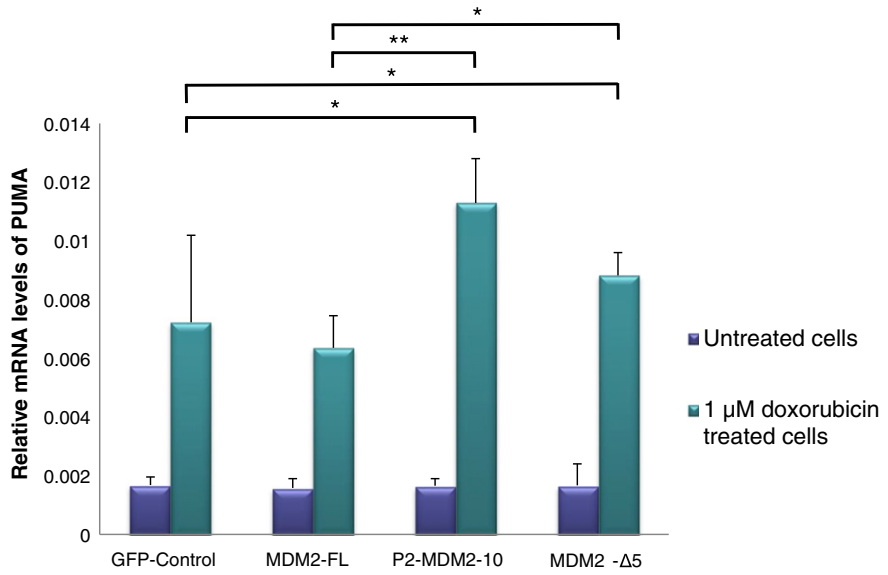

Figure 6. Transactivation of *PUMA* at mRNA level. MCF-7 cells transfected with pCMV-GFP (Control), MDM2-FL, P2-MDM2-10, and MDM2-Δ5, sorted after 12 hours based on GFP expression, followed by treatment with DMSO (purple bars) or 1 μM doxorubicin (green bars) for 24 hours. The experiment was repeated in triplicate, with three independent transfections. *$P \leq .05$, **$P \leq .01$.

ineffective transfection, as mRNA levels were confirmed by qPCR (data not shown).

The same panel of genes as described above for P2- MDM2-10 was examined upon overexpression of MDM2-Δ5. A significant upregulation of *PUMA* compared to the controls ($P = .039$) as well as MDM2-FL–transfected cells ($P = .033$) after doxorubicin treatment was observed (Figure 6); however, none of the other target genes showed significantly altered expression levels.

Moreover, overexpressing MDM2-Δ5 led to increased levels of endogenous *MDM2* mRNA compared to the control cells ($P = .011$; Figure 7). Also, after overexpression of MDM2-Δ5 and concomitant doxorubicin treatment, the levels of endogenous *MDM2* were increased as compared to the control cells, but this difference did not reach statistical significance ($P = .070$).

Examining cell cycle progression in cells overexpressing MDM2-Δ5 with and without chemotherapy, we did not observe any significant difference compared to the control cells (Figure 8*A*). However, similar to P2-MDM2-10, and in line with the induction of *PUMA*, overexpression of MDM2-Δ5 led to a marked increase in the degree of apoptotic cells compared to the GFP-control both in

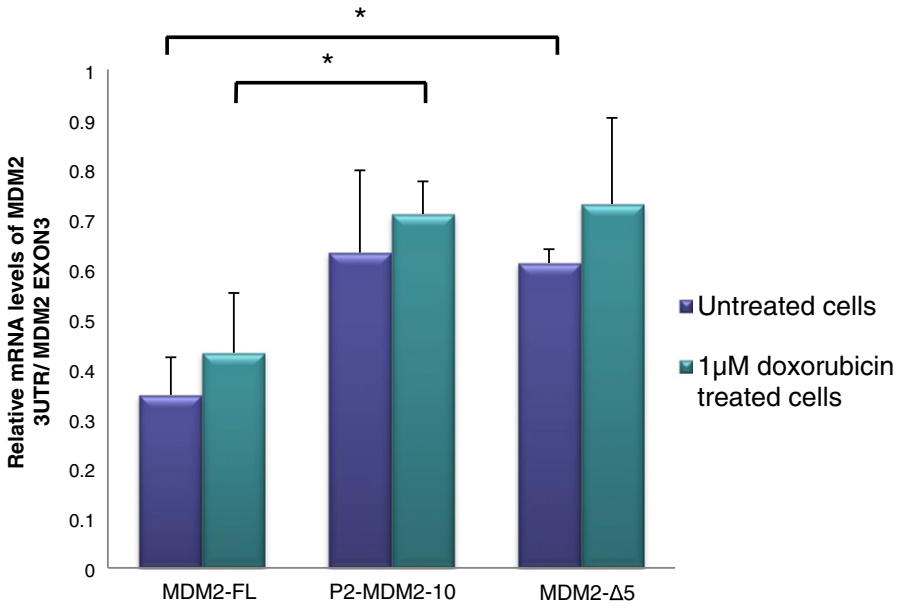

Figure 7. Relative expression of MDM2 after transfection with the *MDM2* splice variants. mRNA levels of MDM2 measured after transfection with MDM2-FL, P2-MDM2-10, and MDM2-Δ5 in MCF-7 cells after sortation by GFP expression, untreated cells (purple bars), or 1 μM doxorubicin–treated (green bars) for 24 hours. The experiment was repeated in triplicate, with three independent transfections. *$P \leq .05$.

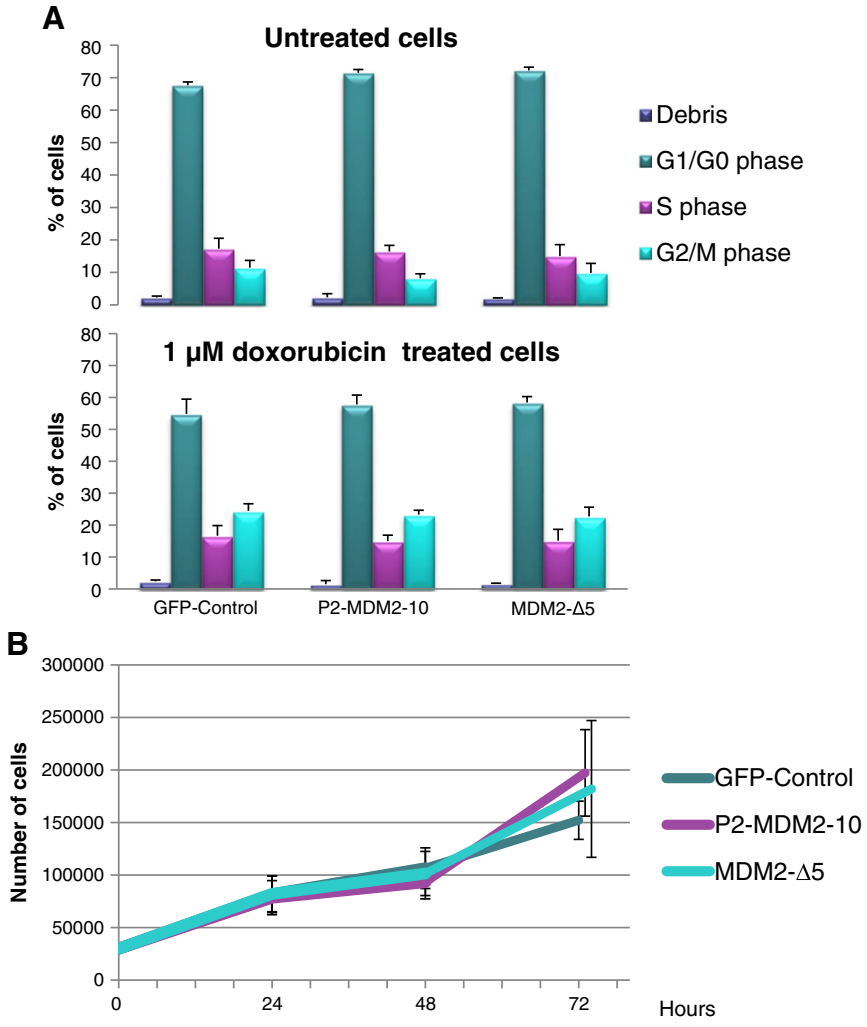

Figure 8. Cell cycle and cell proliferation analysis. (A) Cell cycle analysis of cells overexpressing the splice variants. MCF-7 breast cancer cells were transfected with pCMV-GFP (GFP-control), P2-MDM2-10, and MDM2-Δ5. Twenty-four hours posttransfection, untreated (left panel) or treated with 1 μM doxorubicin (right panel) for 24 hours. The cells were analyzed by NucleoCounter-3000 for status of cell cycle progression. Bars represent cell debris (purple), cells in G1/G0 phase (green), cells in S phase (pink), and cells in G2/M phase (blue) respectively. (B) Cell proliferation analyzed by cell count. MCF-7 breast cancer cells transfected with pCMV-GFP (GFP-control), P2-MDM2-10, and MDM2-Δ5 were counted to examine the cell proliferation 24, 48, and 72 hours posttransfection (data points at 72 hours have been slightly shifted on the *x*-axis of the graph, for clarity). The experiment was repeated in triplicate, with three independent transfections. Error bars indicate standard deviation.

untreated and in doxorubicin-treated cells (51% vs. 28% and 66% vs. 49%, respectively, yet not significantly; Figure 9*A*). Overexpression of MDM2-Δ5 in both HCT116 *TP53*+/+ and HCT116 *TP53*−/− showed indications of increased activation of apoptosis upon doxorubicin treatment; however, it did not reach statistical significance (Figure S5).

Also, similar to the effect of P2-MDM2-10, the increase in number of cells undergoing apoptosis induced by MDM2-Δ5 was accompanied by a reduction in senescent cells upon doxorubicin treatment compared to the TOPO-control (5.8-fold vs. 3.3-fold; Figure 9*B*; *P* for interaction = .027).

Discussion

Previous studies have shown DNA-damaging drugs causing genotoxic stress to promote splice-pattern alterations in *MDM2 in vitro* [29]. While multiple *MDM2* splice variants have been identified, their functional roles are poorly understood. In the present study, we investigated some molecular features of, and the possible biological effects of, the alternative spliced variants P2-MDM2-10 and MDM2-Δ5 in response to chemotherapy treatment in breast cancer cells.

The P2-MDM2-10 variant was reported in 2008, and the authors suggested it to be expressed mainly from the *MDM2* promoter P2 [25]. Contrasting this, we observed the P2-MDM2-10 to be expressed from both promoters (P1 and P2), indicating this variant to be present in cells both in the normal state and under stressed conditions. Further, based on high expression levels in our initial screen, we assessed the potential link between *MDM2* promoter SNP status and the expression levels of P2-MDM2-10 and also included the variant with the second highest occurrence in our large-scale screen, MDM2-Δ5, in our studies.

Under stressed conditions, we observed both of the splice variants to be upregulated, similar to what is observed for MDM2-FL. However, contrasting what has been reported for MDM2-FL [12],

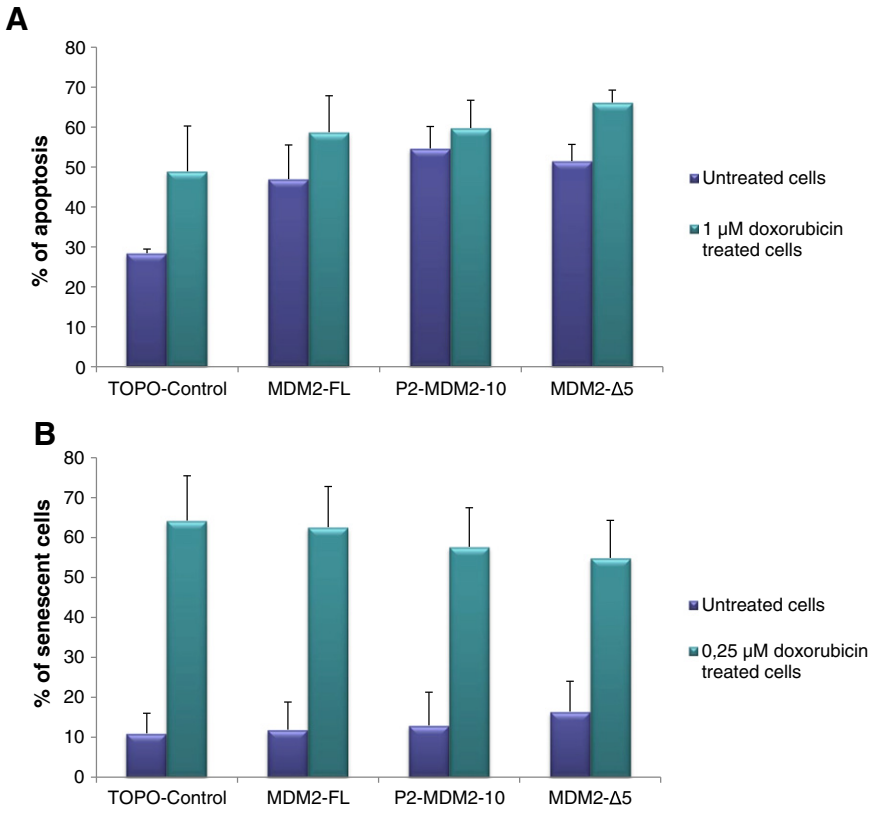

Figure 9. Induction of apoptosis and senescence in MCF-7 cells. (A) Bars illustrate the percentage of apoptotic cells after transfection with pCMV (TOPO-Control), MDM2-FL, and the splice variants, untreated (purple bars) or treated with 1 μM doxorubicin (green bars) and analyzed by Annexin V assay 24 hours post transfection. The bars represent the cells that are both early apoptotic and apoptotic. The experiment was repeated in triplicate with three independent transfections. (B) Graphs illustrate the percentage of senescent cells after transfection with pCMV (TOPO-Control), P2-MDM2-10, and MDM2-Δ5. Untreated (purple bars) or treated with 0.25 μM doxorubicin (green bars) analyzed by β-galactosidase assay 8 days posttransfection. The experiment was repeated in triplicate with three independent transfections.

we found normal tissue expression levels of both splice variants to be higher among individuals harboring the SNP309TT genotype as compared to the SNP309TG and GG genotypes. For P2-MDM2-10, this observation was only significant under unstressed condition, while for MDM2-Δ5, there was a significant difference both under unstressed and under stressed conditions. Given that the SNP309 G-allele in general is thought to increase the expression levels of MDM2-FL, our findings of the opposite result for both of the splice variants examined suggest that P2-MDM2-10 and MDM2-Δ5 both may have biological functions different from the MDM2-FL. Notably, this finding also indicates a potentially more complex role of the *MDM2* promoter SNPs than previously presumed; promoter genotype not only may influence *MDM2* full-length expression level but influence *MDM2* splice variant profile as well.

While we found P2-MDM2-10 to be translated into a protein product, we were unable to detect any protein expression from the MDM2-Δ5 splice variant despite high mRNA levels. Antibodies against both C-terminal and N-terminal for detection of possible transcripts were tested. However, upregulation of MDM2-Δ5 transcripts was observed by qPCR for exon 3, demonstrating successful transfection and possible effect of this splice variant at mRNA level. Thus, the lack of protein does not rule out a biological effect of this variant since it is known that other transcribed variants of *MDM2* that are not translated still are functional [26].

We found the P2-MDM2-10 protein to be markedly more stable than the MDM2-FL protein: While MDM2-FL was completely degraded 4 hours post cycloheximide treatment, P2-MDM2-10 was still present in the cells as a stable protein. This further indicates P2-MDM2-10 to be subject to regulations different from the MDM2-FL. Further, our findings show that the splice variant P2-MDM2-10 is mostly located in the nucleus and not in the cytoplasm. MDM2 binds to p53 by interaction through the amino terminus binding pocket domain, the central acidic domain, and the C-terminal [30]. P2-MDM2-10 has both the p53 binding domain intact and the NLS and NES, explaining the low levels of this splice variant in the cytoplasm due to possible colocalization with p53 into the nucleus and/or by the presence of NLS itself.

After doxorubicin treatment, we found *PUMA* expression to be significantly increased after overexpression of both P2-MDM2-10 and MDM2-Δ5. Even though we did not observe any marked changes in the expression of other genes downstream of p53/MDM2, the *PUMA* upregulation was accompanied by an increase of cells undergoing apoptosis, strongly indicating that both P2-MDM2-10 and MDM2-Δ5 have functional roles linked to the apoptotic program. Interestingly, we found the proapoptotic effect of both P2-MDM2-10 and MDM2-Δ5 to be accompanied by a reduced senescence, and these findings might indicate the splice variants to be involved in a competitive effect/balance between these two processes in response to doxorubicin treatment.

Notably, the impact of the two splice variants on apoptosis resembled the effect observed upon overexpression of MDM2-FL. Thus, contrasting expectations based on current knowledge about MDM2's function degrading p53 [3,31,32], we found overexpression of MDM2-FL, both in the untreated as well as in treated MCF-7 cells, to increase the fraction of apoptotic cells. This finding was substantiated by the finding of no decrease in apoptosis following MDM2-FL overexpression in either HCT116 *TP53*+/+ and HCT116 *TP53*–/– cells, indicating a p53 independent functional effect of exogenous MDM2-FL in our model systems. Although not directly linked to apoptosis, it has previously been found that ectopic expression of MDM2 led to p53 independent genomic instability, with large increases in the dsDNA breaks [33].

Overexpression of both the P2-MDM2-10 and MDM2-Δ5 splice variants induced increased levels of endogenous MDM2-FL. Although the mechanism behind this remains unknown, one may speculate that feedback loops are operative and that the alternative functions of the splice variants are compensated by increased MDM2-FL expression. Further, even though P2-MDM2-10 is observed to be translated into a protein product, while MDM2-Δ5 is not, our results indicate, nevertheless, the two to exert similar biological functions in the cells.

Taken together, our present findings indicate that the *MDM2* splice variants P2-MDM2-10 and MDM2-Δ5 have several features and functions differing from the MDM2-FL, including potentially important roles in regulating key cellular functions such as apoptosis via activation of the proapoptotic gene *PUMA*.

Acknowledgements

We thank Elise de Faveri, Beryl Leirvaag, and Silje Bjørneklett for technical assistance and Einar Birkeland for scientific and technical advice. We also thank The Medical Service, Royal Norwegian Navy, and Norwegian Armed Forces Joint Medical Service for facilitating sample collection.

Funding

This work was performed in the Mohn Cancer Research Laboratory. The project was supported by grants from the Norwegian Cancer Society, the Norwegian Health Region West, and the Bergen Medical Research Foundation.

Conflict of Interest

The authors declare no conflict of interest.

Appendix A. Supplementary data

Supplementary data to this article can be found online at http://dx.doi.org/10.1016/j.tranon.2017.07.006.

References

[1] Momand J, Zambetti GP, Olson DC, George D, and Levine AJ (1992). The mdm-2 oncogene product forms a complex with the p53 protein and inhibits p53-mediated transactivation. *Cell* **69**, 1237–1245.

[2] Fakharzadeh SS, Trusko SP, and George DL (1991). Tumorigenic potential associated with enhanced expression of a gene that is amplified in a mouse tumor cell line. *EMBO J* **10**, 1565–1569.

[3] Haupt Y, Maya R, Kazaz A, and Oren M (1997). Mdm2 promotes the rapid degradation of p53. *Nature* **387**, 296–299.

[4] Honda R, Tanaka H, and Yasuda H (1997). Oncoprotein MDM2 is a ubiquitin ligase E3 for tumor suppressor p53. *FEBS Lett* **420**, 25–27.

[5] Wu X, Bayle JH, Olson D, and Levine AJ (1993). The p53-mdm-2 autoregulatory feedback loop. *Genes Dev* **7**, 1126–1132.

[6] Zauberman A, Barak Y, Ragimov N, Levy N, and Oren M (1993). Sequence-specific DNA binding by p53: identification of target sites and lack of binding to p53 - MDM2 complexes. *EMBO J* **12**, 2799–2808.

[7] Momand J, Jung D, Wilczynski S, and Niland J (1998). The MDM2 gene amplification database. *Nucleic Acids Res* **26**, 3453–3459.

[8] Michael D and Oren M (2002). The p53 and Mdm2 families in cancer. *Curr Opin Genet Dev* **12**, 53–59.

[9] Barak Y, Gottlieb E, Juven-Gershon T, and Oren M (1994). Regulation of mdm2 expression by p53: alternative promoters produce transcripts with nonidentical translation potential. *Genes Dev* **8**, 1739–1749.

[10] Zauberman A, Flusberg D, Haupt Y, Barak Y, and Oren M (1995). A functional p53-responsive intronic promoter is contained within the human mdm2 gene. *Nucleic Acids Res* **23**, 2584–2592.

[11] Mendrysa SM and Perry ME (2000). The p53 tumor suppressor protein does not regulate expression of its own inhibitor, MDM2, except under conditions of stress. *Mol Cell Biol* **20**, 2023–2030.

[12] Bond GL, Hu W, Bond EE, Robins H, Lutzker SG, Arva NC, Bargonetti J, Bartel F, Taubert H, and Wuerl P, et al (2004). A single nucleotide polymorphism in the MDM2 promoter attenuates the p53 tumor suppressor pathway and accelerates tumor formation in humans. *Cell* **119**, 591–602.

[13] Knappskog S, Bjornslett M, Myklebust LM, Huijts PE, Vreeswijk MP, Edvardsen H, Guo Y, Zhang X, Yang M, and Ylisaukko-Oja SK, et al (2011). The MDM2 promoter SNP285C/309G haplotype diminishes Sp1 transcription factor binding and reduces risk for breast and ovarian cancer in Caucasians. *Cancer Cell* **19**, 273–282.

[14] Economopoulos KP and Sergentanis TN (2010). Differential effects of MDM2 SNP309 polymorphism on breast cancer risk along with race: a meta-analysis. *Breast Cancer Res Treat* **120**, 211–216.

[15] Hu Z, Jin G, Wang L, Chen F, Wang X, and Shen H (2007). MDM2 promoter polymorphism SNP309 contributes to tumor susceptibility: evidence from 21 case-control studies. *Cancer Epidemiol Biomark Prev* **16**, 2717–2723.

[16] Gansmo LB, Knappskog S, Romundstad P, Hveem K, Vatten L, and Lonning PE (2015). Influence of MDM2 SNP309 and SNP285 status on the risk of cancer in the breast, prostate, lung and colon. *Int J Cancer* **137**, 96–103.

[17] Knappskog S, Trovik J, Marcickiewicz J, Tingulstad S, Staff AC, MoMaTEC study group, Romundstad P, Hveem K, Vatten L, and Salvesen HB, et al (2012). SNP285C modulates oestrogen receptor/Sp1 binding to the MDM2 promoter and reduces the risk of endometrial but not prostatic cancer. *Eur J Cancer* **48**, 1988–1996.

[18] Bartel F, Taubert H, and Harris LC (2002). Alternative and aberrant splicing of MDM2 mRNA in human cancer. *Cancer Cell* **2**, 9–15.

[19] Chen J, Marechal V, and Levine AJ (1993). Mapping of the p53 and mdm-2 interaction domains. *Mol Cell Biol* **13**, 4107–4114.

[20] Freedman DA, Epstein CB, Roth JC, and Levine AJ (1997). A genetic approach to mapping the p53 binding site in the MDM2 protein. *Mol Med* **3**, 248–259.

[21] Momand J, Villegas A, and Belyi VA (2011). The evolution of MDM2 family genes. *Gene* **486**, 23–30.

[22] Freedman DA, Wu L, and Levine AJ (1999). Functions of the MDM2 oncoprotein. *Cell Mol Life Sci* **55**, 96–107.

[23] Roth J, Dobbelstein M, Freedman DA, Shenk T, and Levine AJ (1998). Nucleo-cytoplasmic shuttling of the hdm2 oncoprotein regulates the levels of the p53 protein via a pathway used by the human immunodeficiency virus rev protein. *EMBO J* **17**, 554–564.

[24] Sigalas I, Calvert AH, Anderson JJ, Neal DE, and Lunec J (1996). Alternatively spliced mdm2 transcripts with loss of p53 binding domain sequences: transforming ability and frequent detection in human cancer. *Nat Med* **2**, 912–917.

[25] Arva NC, Talbott KE, Okoro DR, Brekman A, Qiu WG, and Bargonetti J (2008). Disruption of the p53-Mdm2 complex by Nutlin-3 reveals different cancer cell phenotypes. *Ethn Dis* **18** [S2-1-8].

[26] Bartl S, Ban J, Weninger H, Jug G, and Kovar H (2003). A small nuclear RNA, hdm365, is the major processing product of the human mdm2 gene. *Nucleic Acids Res* **31**, 1136–1147.

[27] Sam KK, Gan CP, Yee PS, Chong CE, Lim KP, Karen-Ng LP, Chang WS, Nathan S, Rahman ZA, and Ismail SM, et al (2012). Novel MDM2 splice variants identified from oral squamous cell carcinoma. *Oral Oncol* **48**, 1128–1135.

[28] Knappskog S, Gansmo LB, Romundstad P, Bjornslett M, Trovik J, Sommerfelt-Pettersen J, Lokkevik E, N.V. Norwegian Breast Cancer Group trial, Tollenaar RA, and Seynaeve C, et al (2012). MDM2 promoter SNP344T>A (rs1196333) status does not affect cancer risk. *PLoS One* **7**, e36263.

[29] Chandler DS, Singh RK, Caldwell LC, Bitler JL, and Lozano G (2006). Genotoxic stress induces coordinately regulated alternative splicing of the p53 modulators MDM2 and MDM4. *Cancer Res* **66**, 9502–9508.

[30] Poyurovsky MV, Katz C, Laptenko O, Beckerman R, Lokshin M, Ahn J, Byeon IJ, Gabizon R, Mattia M, and Zupnick A, et al (2010). The C terminus of p53 binds the N-terminal domain of MDM2. *Nat Struct Mol Biol* **17**, 982–989.

[31] Honda R and Yasuda H (2000). Activity of MDM2, a ubiquitin ligase, toward p53 or itself is dependent on the RING finger domain of the ligase. *Oncogene* **19**, 1473–1476.

[32] Wade M, Li YC, and Wahl GM (2013). MDM2, MDMX and p53 in oncogenesis and cancer therapy. *Nat Rev Cancer* **13**, 83–96.

[33] Bouska A, Lushnikova T, Plaza S, and Eischen CM (2008). Mdm2 promotes genetic instability and transformation independent of p53. *Mol Cell Biol* **28**, 4862–4874.